

# Single-cell approaches for studying the role of mitochondrial DNA in neurodegenerative disease

Bailey, Laura J; Elson, Joanna L; Pienaar, Ilse

DOI:

[10.1007/978-1-0716-1270-5\\_19](https://doi.org/10.1007/978-1-0716-1270-5_19)

License:

Other (please specify with Rights Statement)

*Document Version*

Peer reviewed version

*Citation for published version (Harvard):*

Bailey, LJ, Elson, JL & Pienaar, I 2021, Single-cell approaches for studying the role of mitochondrial DNA in neurodegenerative disease. in V Weissig & M Edeas (eds), *Mitochondrial Medicine: Volume 3: Manipulating Mitochondria and Disease- Specific Approaches*. 2 edn, Methods in molecular biology (Clifton, N.J.), vol. 2277, pp. 299-329. [https://doi.org/10.1007/978-1-0716-1270-5\\_19](https://doi.org/10.1007/978-1-0716-1270-5_19)

[Link to publication on Research at Birmingham portal](#)

**Publisher Rights Statement:**

Post-prints are subject to Springer Nature re-use terms <https://www.springernature.com/gp/open-research/policies/accepted-manuscript-terms>

**General rights**

Unless a licence is specified above, all rights (including copyright and moral rights) in this document are retained by the authors and/or the copyright holders. The express permission of the copyright holder must be obtained for any use of this material other than for purposes permitted by law.

- Users may freely distribute the URL that is used to identify this publication.
- Users may download and/or print one copy of the publication from the University of Birmingham research portal for the purpose of private study or non-commercial research.
- User may use extracts from the document in line with the concept of 'fair dealing' under the Copyright, Designs and Patents Act 1988 (?)
- Users may not further distribute the material nor use it for the purposes of commercial gain.

Where a licence is displayed above, please note the terms and conditions of the licence govern your use of this document.

When citing, please reference the published version.

**Take down policy**

While the University of Birmingham exercises care and attention in making items available there are rare occasions when an item has been uploaded in error or has been deemed to be commercially or otherwise sensitive.

If you believe that this is the case for this document, please contact [UBIRA@lists.bham.ac.uk](mailto:UBIRA@lists.bham.ac.uk) providing details and we will remove access to the work immediately and investigate.

# Single Cell Approaches for Studying the Role of Mitochondrial DNA in Neurodegenerative Disease

Laura J. Bailey<sup>1</sup>, Joanna L. Elson<sup>2</sup> and Ilse S. Pienaar<sup>1</sup>

1. Genome Damage and Stability Centre, School of Life Sciences, University of Sussex, Falmer, United Kingdom, BN1 9RQ
2. Institute of Genetic Medicine, Newcastle University, Newcastle-upon-Tyne, United Kingdom, NE1 3BZ
3. School of Life Sciences, University of Sussex, Falmer, United Kingdom, BN1 9PH

**Running head:** Single Cell Approaches for Studying Mitochondrial DNA

## **Abstract**

In light of accumulating evidence suggestive of cell type-specific vulnerabilities as a result of normal aging processes that adversely affect the brain, as well as age-related neurodegenerative disorders such as Parkinson's disease (PD), the current chapter highlights how we study mitochondrial DNA (mtDNA) changes at a single cell level. In particular, we comment on increasing questioning of the narrow neurocentric view of such pathologies, where microglia and astrocytes have traditionally been considered bystanders rather than players in related pathological processes. Here we review the contribution made by single cell mtDNA alterations towards neuronal vulnerability seen in neurodegenerative disorders, focusing on PD as a prominent example. In addition, we give an overview of methodologies that support such experimental investigations. In considering the significant advances that have been made in recent times for developing mitochondria-specific therapies, investigations to account for cell type-specific mitochondrial patterns and how these are altered by disease, hold promise for delivering more effective disease-modifying therapeutics.

**Key words** Age-related disorders, Cell specificity, Mitochondria, Mitochondrial DNA, Neurodegeneration, Parkinson's disease, Single cell analyses

## **1 Introduction**

Recent years have seen a rapid development of technologies and methods that permit a detailed analysis of the genome and transcriptome of a single cell. This experimental approach has enabled systematic investigation of cellular heterogeneity in a wide range of tissue types and cell populations, yielding fresh insights into the composition, dynamics and regulatory mechanisms of cell states, reflective of stages of organism development but also of disease.

Application of a single cell methodology is particularly important for studying the role played by defective mitochondria in human diseases. Mitochondria comprise of small cytosolic organelles which evolved as a result of a symbiotic relationship that developed 1.5 billion years ago between primordial eukaryotic cells and aerobic bacteria [1]. A permanent relationship was established when such bacteria developed into organelles, for providing the host cells with aerobic metabolism, while, in turn, the organelles adapted to the new intracellular environment by reducing their genome size. This reduction in genome size resulted in the loss of their ability to exist independent of their host.

## **2 Mitochondrial DNA encoding content and its maintenance**

Mitochondrial DNA (mtDNA) comprise of a 16,569-kb circular, double-stranded molecule. The two strands of mtDNA differ in their nucleotide composition, with a cytosine-rich light (L) and guanine-rich heavy (H) strand. MtDNA contains 37 genes, consisting of two ribosomal RNA (rRNA) genes for protein synthesis, 22 transfer RNA (tRNA) genes and also 13 protein coding genes. These encode proteins that form the core of four of the five multi-subunit protein complexes of the mitochondrial electron transport chain (ETC), namely complex I, III, IV and V. All the other proteins required to construct and maintain mitochondria are

nuclear encoded, as well as the entirety of complex II of the ETC. The ETC is located within the mitochondrial inner membrane. Via oxidation of the co-enzyme NADH (nicotinamide adenine dinucleotide) the ETC delivers the energy needed to synthesise ATP, thereby providing almost all of the cell's energy requirements by means of transference of electrons to oxygen [2]. However, as functional units, mitochondria not only serve to supply a cell's energy demands, but also fulfill roles in apoptosis [3] and calcium regulation [4].

Even in light of this small number of genes, mammalian mtDNA is strikingly compact since, unlike the nuclear genome, it contains no introns, while genes in some cases even partially overlap. The whole molecule is transcribed poly-cistronically before being processed to add additionally required features such as polyadenylation [5]. MtDNA also encompass two non-coding regions (NCR) sized at 700 bp in mice and 1,100 in humans. The NCR is the largest of the two, at 1,124-bp, and contains the promoters for transcription of both the H and L strands of mtDNA. Strikingly, the NCR contains a complex structure consisting of several additional strands of nucleic acids, which are found in varying abundance. The first of these to be identified was a short DNA strand known as the 7S DNA, an approximately 0.5 kb DNA molecule located to within the NCR [6].

The role of the displacement (D)-loop, a triple-stranded region occurring within the main NCR of most mitochondrial genomes, is formed through stable incorporation of 7S DNA [7]. The function of this region is still not fully understood, although it's been shown to have important roles in mtDNA organization, segregation and replication [7-9], yet its abundance was found to vary greatly across cell lines and tissue types [10]. More recently a second molecule has been found in this region, namely the LC-RNA (light- (or lagging-) strand, CR RNA) that is complimentary to 7S DNA. This RNA molecule is believed important for regulating transcription of the mtDNA molecule [11, 12]. A much smaller, but also important

regulatory region of the mitochondrial genome, termed the origin of light strand replication ( $O_L$ ), contains the origin of replication of the L strand, with this region forming a stem loop structure when it becomes single stranded, due to replication on the leading strand, and also allows replication to be initiated in the opposite direction [13, 14]. Due to the essential nature of these regions for the maintenance of the mtDNA molecule, deletions and mutations are rarely seen in these regions.

### **3 MtDNA copy number and the threshold effect**

Unlike nuclear DNA, mtDNA molecules exist in multiple copies per cell, varying between as much  $10^3$ - $10^4$  mtDNA copies per cell (also referred to as copy number (CN)), depending on a particular cell's bioenergetic demands. MtDNA replicates independently of the cell cycle, termed 'relaxed replication', with this process occurring in both dividing and non-dividing cells. Any one mtDNA molecule might be copied multiple times or not at all during the process of mtDNA CN maintenance. MtDNA CN can change in relation to nuclear DNA levels and is regulated by mitochondrial proteins such as TFAM (transcription factor A, mitochondrial) and POLG (polymerase  $\gamma$ ). In healthy adult brains, the number of mtDNA molecules, or mtDNA CN, varies between different cell types. mtDNA CN is relatively high in neurons, due to the exceedingly high energy demand posed by the brain.

These mtDNA copies are normally homoplasmic, meaning identical throughout the cell. However, when mutations occur, mtDNA within a single cell can be a mixture of normal and mutated copies, termed heteroplasmy. Typically, where heteroplasmy occurs, the same mutated mtDNA molecules tend to occur. When the number of mtDNA copies containing mutations within a cell exceed an arbitrary cut-off point (~60%), a functional deficit is expected to occur, manifesting principally as changes in energy production.

#### **4 The role of mtDNA changes in normal aging and in age-related neurodegenerative disease**

There is mounting evidence to suggest that mtDNA damage plays an important role in the pathological processes underlying normal aging as well as age-associated neurodegenerative disease. MtDNA damage is frequently seen to accumulate in somatic cells with age [15], being more prevalent in patients suffering from neurodegenerative disease than in neurological control patients [16]. Once mutated mtDNA molecules have reached a threshold of 60-90% within a cell, a biochemical defect is usually detectable as reduced activity of cytochrome c oxidase (COX), the terminal oxidase of the mitochondrial ETC in mammals [17]. When the observation of COX-negative cells in aged individuals were first made, tissue homogenates was used to consider mtDNA damage [18]. Using this methodology (that is based on tissue homogenates), many of the mtDNA mutations were seen at low levels. However, it was unclear whether all the mutations were at a low level across all cells, or whether each affected cell contains its own mutation at a higher level. This led some to suggest the 'vicious cycle' hypothesis [16]. The premise of the 'vicious cycle' hypothesis was that mtDNA lies in close proximity to the ETC, a source of free radicals, with free radicals being DNA damaging agents. This damaged mtDNA produces damaged ETC proteins that result in increased generation of free radicals, thereby creating further mtDNA damage. The prediction of the vicious cycle hypothesis is that cells showing respiratory chain defects in aged individuals would contain a plethora of different mtDNA mutations.

Understanding the contribution made by neuronal biochemical defects that stem from mtDNA alterations in normal aging is continuously being updated, with the finding that different cells seemingly contain different mutations, where the mutation might be either a point mutation or deletion, but its apparent that each cell contains one dominant mutation

species only [19]. Such results support the theory that a mutated mtDNA molecule undergoing clonal expansion, to eventually outnumber its wild-type (w/t) mtDNA counterpart and become the dominant allele within a cell, can result in the cell experiencing a biochemical defect [20]. The process of clonal expansion is possible due to relaxed replication, and has been suggested to be enhanced by a process called the 'maintenance of wild-type', whereby a cell upregulates mtDNA replication in an attempt to restore the optimal mtDNA CN when facing a large number of somatic mutations [21]. These observations using single cell investigative methodologies brought an end to the 'vicious cycle' hypothesis as a way to explain the accumulation of mtDNA damage with increased age. It remains unclear whether mutant mtDNA molecules proliferate due to some select advantage afforded under certain circumstances, or if random genetic drift is sufficient to explain the accumulation of respiratory-deficient cells with age. One critical observation driving this discussion relates to studies investigating clonal expansion in short-lived animals such as mice, where such animals do not live for long enough time periods that would allow for clonal expansion of levels sufficient for generating a severe biochemical defect [22].

Investigations at a single cell level has provided us with vital understanding as to the distribution of mtDNA mutations and their impact on human health. This technology is being used increasingly to better understand different cell types' specific vulnerabilities to mtDNA-related disease processes, and also the differences between neuronal types in the response to accumulation of somatic mtDNA mutations.

#### **4.1 Susceptibility of mtDNA in Parkinson's disease: A growing realization for cell type specific variation**



A case in point for application of methodologies for assessing the extent of mtDNA variation and its biochemical and physiological consequences relates to investigations concerning Parkinson's disease (PD), a progressive neurodegenerative disease that transcends into a manifestation of both motor and non-motor symptoms [23, 24]. Although principally regarded as a motor disorder, with muscular rigidity, tremor at rest and bradykinesia that form the cardinal features, it is becoming increasingly recognised that non-motor features of the disease can be significantly more debilitating and resistant to treatments than the motor aspects. PD-related non-motor symptoms are diverse and include dementia, mild cognitive impairment, psychosis, apathy, restlessness (akathisia) and impulse control disorders, as well as depression, anxiety, sleep disorders, orthostatic hypotension, constipation and pain. Such symptoms can be localized to the cortex, basal ganglia, brainstem, spinal cord and peripheral nervous system.

It is now well established that the cardinal motor symptoms of PD are due to the death of dopaminergic neurons in the Substantia Nigra pars compacta (SNpc), a midbrain nucleus that forms part of the basal ganglia circuitry, which fulfills a critical role in modulating motor movement and reward functions [25]. A further core neuropathological characteristic of PD brains is the presence of Lewy bodies (LBs) and Lewy neurites (LNs) containing abnormal misfolded protein aggregates, including  $\alpha$ -synuclein ( $\alpha$ -SYN) that accumulate intracellularly [26] and has been proposed to progress through the brain caudo-rostrally [27]. In this regard, accumulating convincing evidence suggests for the prion-like qualities of the  $\alpha$ -SYN protein due to the neuron-to-neuron transfer noted in grafted neurons transplanted in PD patient brains over a decade prior to autopsy [28], in cell culture [29, 30], and also in experimental animal models [31]. In PD patients, LB progression throughout the brain has also been correlated with disease severity [27]. However, whether these intracellular inclusions

comprise a pathological substrate of the clinical syndrome of PD, or whether their presence rather indicates neuroprotection, remains to be determined. Regardless of this ongoing debate, the notion of PD being regarded as a synucleinopathy now seems firmly established.

Over recent years it has become increasingly apparent that degeneration of neurons and the formation of abnormal protein aggregates within the remaining neurons of PD patient brains are not limited to the SNpc dopaminergic neurons, thereby sparking significant interest as to the degree of involvement of cholinergic, serotonergic, noradrenergic and other neurotransmitter systems, which provide the neural substrate for several PD-associated symptoms. In this regard, evidence was given that dysfunction and/or degeneration of regions such as the locus coeruleus (LC) and dorsal raphe nucleus, the main sources of norepinephrine and serotonin (5-hydroxytryptamine; 5-HT), respectively, in the brain, contribute especially to 'axial' symptoms and also cognitive impairment. Another brain region and neuronal type that has gained prominence as another likely cause of disability during disease evolution in PD are the large 'Ch5' cholinergic neurons of a brainstem nucleus, the pedunculo-pontine nucleus (PPN) [32-35]. Although other cell types, including glutamatergic, GABAergic and glycinergic neurons (that may co-express a variety of neuropeptides) locating to this heterogeneous nucleus may also be lost during PD progression [36-42], the resident cholinergic population remains the most severely affected [41], where a PPN cholinergic lesion induces dysfunctions in the complex neural network that the PPN forms a key component of.

Reasons that render the SNpc dopaminergic and PPN cholinergic neurons particularly vulnerable to PD disease processes remain to be fully determined; however, striking similarities deemed to be important contributing factors are noted between these two neural structures, including the very long neuronal projections and extensive arborisations inherent to

both SNpc dopaminergic and PPN cholinergic neurons. In each case, a far less dense portion containing other types of neurons is also present, with such neurons containing a far more restricted projection profile compared to the adversely impacted dopaminergic or cholinergic neurons [43].

Other inherent factors that may explain (or at least contribute) to the selective vulnerability of certain cell populations include dysfunctional brain iron metabolism, particularly affecting the uptake, storage and release of iron [44]. In particular, iron-related mechanisms have been deemed potentially important for the large-scale cell death affecting nigral dopaminergic neurons, as well as the tendency for remaining ones to undergo  $\alpha$ -SYN aggregation, lending support to the use of iron chelator drugs as a promising therapeutic strategy for PD [45]. A plausible mechanism by which nigral dopaminergic neurons, in particular, are susceptible to excessive iron deposition may relate to interaction of iron with neuromelanin, a dark coloured granular pigment present in this neuronal group [46]. Shamoto-Nagai and others [47] provided some details as to this interaction by showing that iron released from neuromelanin increases oxidative stress within the mitochondria, thereby causing mitochondrial dysfunction and, in turn, reduce proteasome function. Whether altered iron levels associate with loss of other cells that lie outside the SNpc remains largely unexplored, with only the LC that has been explored in this regard, showing no such association [48, 49].

The diversity of cell types affected during PD pathogenesis go far to explain the wide range of symptoms displayed by PD patients, while providing multiple targets for pharmacological interventions to treat such symptoms. Brain vasculature is a non-neuronal cell type that may also be affected during PD. For instance, our group reported extensive damage affecting microvessels within the subthalamic nucleus (STN), as was assessed in post-mortem PD brains [50]. In particular, we found striking downregulation of vascular adherens

junction, tight junction-associated proteins and also vascular endothelial growth factor (VEGF) in PD-afflicted brains compared to neurological controls, as well as several adverse structural alterations in the PD samples, including severe thinning of microvessel endothelial cell thickness and also shortening of such vessels. Interestingly, this research also demonstrated that a surgical therapeutic intervention termed deep-brain stimulation (DBS) greatly improved these cellular and molecular aspects in PD patients when compared to PD patients that did not receive STN-DBS.

Astrocytes, comprising the most populous glial subtype is a brain residing cell type that has received significantly less research attention with regards to a possible role in PD [51]. As critical regulators of a variety of brain functions, they provide structural and metabolic support, and also regulate synaptic transmission, water transportation and blood flow within the brain [52]. Recent evidence indicated that disrupted astrocyte biology might have a fundamental role in neuronal degeneration seen in the brains of PD patients. In this regard, monogenetic mutations affecting 17 genes that have been implicated in the development of the disease were found expressed in the astrocytes of different human and mouse brains, in some instances higher than was seen in neurons [53].

Moreover, evidence suggesting an immune response in the brains of PD patients has increased greatly, to implicate microglia cells that play a major role in the inflammatory process, by rapidly responding in a phagocytic manner to pathological insults [54, 55]. Recently, George and others [56] reported that microglia, when activated due to pro-inflammatory stimuli, increasingly partake in  $\alpha$ -syn cell-to-cell transfer, thereby promoting prion-like spread of the pathology. Such results suggest that modulation of the innate immune system might mitigate formation and accumulation of intracellular misfolded protein aggregates, which characterizes the brains of PD patients.

PD has a multifactorial etiology, with a variety of genes and molecular pathways that may contribute to the development and progression of this disease, including those involving mitochondria, the organelle providing the majority of cellular energy via adenosine triphosphate (ATP) production. As neurons require high energy levels to maintain intracellular ion concentrations, often against membrane concentration gradients, an impairment to mitochondrial-derived energy could lead to neuronal dysfunction and even cell death. The link between mitochondrial dysfunction and PD was first investigated in the 1970s when MPTP (1-methyl-4-phenyl-1,2,3,6-tetrahydropyridine), a prodrug to the dopaminergic-targeting neurotoxin MPP<sup>+</sup> (1-methyl-4-phenylpyridinium), was found to induce a condition resembling idiopathic PD in drug users [57]. A variety of toxic mechanisms has since been proposed to explain the killing of dopaminergic-specific neurons [58]. However, the main mechanism involves inhibiting mitochondrial complex I, present within the inner mitochondrial membrane [59]. Complex I comprises the first component of the ETC, responsible for generating ATP via a series of redox reactions for oxidative phosphorylation (OXPHOS).

A strong case for mitochondrial damage in PD pathogenesis derives from an extensive body of literature using neurotoxin animal models of PD, where animals reflect core clinical and post-mortem neuropathological features of clinical PD to a remarkably accurate extent. Previously the dopamine transporter (DAT) was deemed to play a crucial role in the dopaminergic-specific toxicity of MPP<sup>+</sup> [60, 61]. However, although it's been known for some time that MPP<sup>+</sup> also acts as a high affinity substrate for the serotonin transporter, which helps explain the MPP<sup>+</sup>-induced damage sustained by the serotonergic neurons, recent findings reported by Martí and others [62] found that MPP<sup>+</sup>'s toxic mechanism-of-action differs between these two monoaminergic neuronal types, particularly relating to differential effects on neurotransmitter release and re-uptake.

Human post-mortem PD tissue analyses revealed depletion of 5-HT levels within serotonergic neurons that originate from the raphe nuclei [27]. The additional finding of significant variance of 5-HT levels across patients, with the concentrations of some PD patients that fell within the range of healthy controls [63, 64] suggests for differential susceptibility towards PD-related pathological processes between these two neuronal types. Although MPP+ is a high affinity substrate for DAT, rendering dopaminergic neurons susceptible to MPP+'s neurotoxic effects [65], the toxin also has affinity (although comparatively lower) for the serotonin transporter, meaning that serotonergic neurons are also vulnerable to MPP+-induced neurotoxicity [62]. However, the vast bulk of MPP+ PD modeling experiments have been performed on dopaminergic-type neurons, leaving the question of whether 5-HT neurons might be less susceptible to MPP+ toxicity, and the mechanisms that might underlie such neuroprotection, largely unanswered. The study by Martí and colleagues [62] enlightened on possible differences to explain the differential susceptibilities by treating stem cell-derived dopaminergic and serotonergic neurons *in vitro*. Whereas MPP+ exposure impaired mitochondrial membrane potential in both cell types, only dopaminergic neurons were affected in terms of 'synaptic vesicle cycling', a molecular process entailing constant recycling of synaptic vesicle protein complexes for effective neurotransmitter release. This result, along with the finding of contrasting differences in MPP+-induced trafficking of neurotransmitter transporter proteins between the two monoaminergic neuronal types indicates that mitochondria metabolism is similarly affected by the toxin treatment, but that the PD-relevant mitochondrial toxin MPP+ exerts different effects on neurotransmitter release and re-uptake, depending on the neuronal type.

Another neurotoxin utilized in PD research, for elucidating on neuropathological mechanisms that converge to adversely affect mitochondrial functions in neurons selectively

vulnerable to PD, is the piscicide, rotenone. By also blocking complex I of the ETC, rotenone exposure results in a loss of ATP synthesis, in a manner similar to MPP+ [66], although later work revealed that bioenergetic defects induced by rotenone exposure are not responsible for cell death [67]. Characterisation of the rotenone rat model of PD substantiated involvement of pesticide exposure and systemic ETC complex I dysfunction in PD's aetiology, with rotenone-treated rats that feature several motor symptoms of PD such as resting tremor and muscle rigidity. In addition, animals treated with rotenone show overlapping cellular pathologies with clinical PD, including selective nigrostriatal dopaminergic degeneration and  $\alpha$ -SYN-positive cytoplasmic inclusions [68]. The MPTP mouse and rotenone rat models are examples of relevant preclinical animal models that reproduce PD pathology with high fidelity. The fact that pathological processes converging on mitochondrial functions are identified consistently as critical mechanisms underlying the pathological profile these animals present with, provide firm evidence that altered mitochondria are key players in progressive PD.

Extensive additional evidence for defective mitochondria's role in PD pathogenesis derives from the consistent link seen between oxidative stress and monogenically inherited PD-associated genes. Whilst most cases of PD (~90%) are sporadic, of the nuclear genes identified to play a causative role in familial forms of PD, several are known to encode mitochondrial proteins. These proteins form components involved in pathways that are vital for balancing mitochondrial numbers through biogenesis and mitophagy (the process of selectively degrading mitochondria that have been made defective due to damage or stress). Mutations to the nuclear genes *PINK1*, *DJ* and *PARK2* can also directly compromise the rate of OXPHOS [69]. Several genes linked to PD have also been implicated in mechanisms underlying mitochondrial response to stress and autophagy [70]. Mitochondrial dysfunction has also been observed at the early stages of PD progression [70] with defects in mitochondrial

function causing impaired respiratory chain complex I in SNpc dopaminergic neurons [69]. This has led to the proposal of mitochondrial dysfunction and, consequently oxidative stress, through increased generation of ROS, as a contributory factor in the etiology of PD.

In the section above we highlighted work showing that mitochondrial dysfunction and oxidative stress associates with neuronal loss that characterizes PD-affected brains [71] and the multitude of studies which reported the presence of a deficient mitochondrial ETC complex I in remaining brain cells of PD patients [72-74]. In addition, we discussed evidence that inhibitors of complex I of the mitochondrial ETC results in parkinsonism [65], to further corroborate the now established belief that defects in mitochondrial respiration are implicated in the etiology and pathogenesis of PD. The next section will focus more specifically on mtDNA somatic changes in neuronal types deemed important in PD's neuropathology.

MtDNA deletions and mtDNA CN changes have been widely associated with susceptibility to and progression of neurodegenerative disease, including PD [75]. This has been extensively described in one neuronal population that is vulnerable to degeneration in PD, namely the dopaminergic neurons whose cell bodies exist in the SNpc. In one such study, Swerdlow and others [76] reported that an ETC complex I defect can be transferred to cell lines by expressing mtDNA taken from PD patients, implicating somatically acquired lesions affecting the mitochondrial genome in PD pathogenesis. Additional evidence in support of this relates to findings that the SNpc of post-mortem PD patients harbour substantial levels of the types of mtDNA deletions frequently seen in aged brains [77, 78].

Increased large-scale mtDNA deletions were reported as being present in post-mortem PD-affected dopaminergic neurons of the SNpc [79-81]. Such neurons also displayed reduced mtDNA CN [82], thus reducing the pool of w/t mtDNA, which would normally increase with age as compensation for accrued damage over time [82]. In all such studies it is



important to consider age-matched controls in these studies, as ageing is considered the biggest risk factor for PD, with post-mitotic neurons inherently vulnerable to age related decline. The findings from such carefully controlled post-mortem studies have supported the hypothesis that accumulation of such somatically produced mtDNA deletions may eventually cause a bioenergetic deficit, thereby contributing to PD-related neurodegeneration, with this postulation that received indirect support from studies done on mice harboring a mtDNA deficiency within the nigral neurons, where such animals showed a parkinsonian phenotype [83].

Ongoing efforts by our lab and others to identify the nature and spectrum of mtDNA changes affecting different cell types as a consequence of PD pathology, could facilitate the discovery of earlier pathophysiological markers, along with more targeted therapeutic strategies. Studies on post-mortem human brain tissue have shown reduced mtDNA CN in SNpc dopaminergic neurons [70]. Another study reported that mtDNA CN did not significantly differ between SNpc neurons in PD brains with LBs compared to those without LBs [84]. In contrast, cholinergic PPN neurons show elevated mtDNA CN [35]. Interestingly, studies on both nigral dopaminergic and brainstem cholinergic neurons demonstrated increased rates of deletions in mtDNA in PD compared to healthy neurological controls [35].

As neurons, particularly excitatory neurons such as dopaminergic and also cholinergic ones, require high levels of energy to allow ions to pass through their cellular membranes, any defects in energy production could result in impaired neuronal function, manifesting as disease symptoms. SNpc dopaminergic neurons are particularly prone to mitochondrial dysfunction, which could take the form of reduced mitochondrial ETC protein expression and related activity [65], and/or ROS-mediated damage. However, few studies have been done to date for determining the extent and nature of mitochondrial dysfunction in other, non-

dopaminergic cell types implicated in PD pathogenesis. This is an area of research that should be expanded upon to help in designing cell-specific strategies for combatting PD. Recent work examined single cholinergic neurons taken from post-mortem PD brains, to compare to those from control brains [35]. Similar to past studies on nigral dopaminergic neurons, this study reported increased levels of mtDNA deletions in the PD cases compared to the controls. However, in contrast to the studies focused on analysis of the dopaminergic neurons, Bury and others [35] found an elevated mtDNA CN in single PPN cholinergic neurons of the PD cohort, relative to neurological controls. An increase in mtDNA CN could serve as an effort to maintain the w/t mtDNA populations and rescue mitochondrial function within cholinergic neurons [35] and thus the study supports the maintenance of wild-type theory [21].

Metabolic changes may be a contributing factor in the accumulation of mtDNA deletions within neurons. For instance, metabolism of catecholamine, a key synapse-based communication currency for several neuronal types (including dopaminergic neurons), is altered as a result of PD pathology. In this regard, recent *in vitro* and *in vivo* studies, Neuhaus and colleagues [85] provided experimental data to propose that altered catecholamine metabolism due to PD neuropathological processes, could drive the accumulation of mtDNA deletions observed in SNpc dopaminergic neurons of aged brains, with this phenomenon that is exaggerated in PD. In one experiment, the investigators showed in mouse brains, a preference for mtDNA deletions to accumulate within dopaminergic regions such as the SN, striatum and cortex, compared to the cerebellum, a brain region void of dopaminergic somas or terminals. The results concluded that brain regions residing high dopamine metabolism preferentially accumulate mtDNA deletions. Whether a similar principle might underlie the preferential accumulation of mtDNA deletions in other non-dopaminergic neurons during

progressive PD, and if such a phenomenon varies across brain regions, will require similar comparative analyses, e.g. with investigations focusing on cholinergic neurons producing the neurotransmitter acetylcholine (ACh).

Studies to explain the mechanistic basis for differences in the pattern of mtDNA variation between various cell types in PD-affected brains promise to help identify therapeutic targets to exploit in pharmacological screens. In this regard, an accumulating body of work suggests the neuroprotective potential of such mitochondria-targeting therapeutic strategies to influence the course of neurodegenerative disease, as was recently reviewed [86]. Examples of mitochondria-targeted therapeutics for alleviating or even preventing accumulation of mtDNA defects include antioxidant therapy, as well as pharmacological modulators of mitochondrial dynamics.

## **5 Experimental methods for exploring cell-specific brain pathology**

Brain tissue contains different types of neurons and supporting cells, with each type of cell having different functions and molecular compositions. Methods for precisely isolating cells from the surrounding tissue, promise to uncover the spectrum of cell types in the brain and their individual molecular profiles that would otherwise be obscured by whole-tissue approaches. Cell sorting techniques for distinguishing between different cells within tissue can be undertaken in several ways, many of which are becoming cheaper, easier and faster. Traditional techniques include fluorescence-activated cell sorting and laser capture microdissection, while techniques which allow for improved study of the genome, epigenome and transcriptome at single cell resolution are also being developed.

Application of single cell techniques to postmortem tissues can pose significant technical challenges, due to the age or fragility of samples. For example, tissue samples may

have been frozen for many years and therefore ways need to be devised to stabilize the cellular membrane for cell sorting. However, significant progress has been made in this area, and there is now a wealth of published methods and a number of specialist labs developing these to be accessible for all.

### **5.1 Tissue preparation, positive identification of cell types and cell isolation for downstream applications**

Non-fixed, frozen brain blocks containing the region of interest (ROI) should be cut at a thickness optimal for the cell isolator system to be applied to effectively. Sections should be placed on slides of the type best suited for the type of cell isolation apparatus to be used. For instance, laser capture microdissection (LCM) systems comprise of either a “drop-down” or a “catapult” design, where the drop-down version requires slides where tissue sections are placed on a thin plastic membrane, while the catapult version entails placing the sections on non-adhesive glass slides for the cell’s easy removal from the surrounding tissue. For downstream molecular applications involving analysis of DNA or RNA, every effort should be made during the tissue handling process to prevent the degrading influences of RNAases and DNAases, i.e. by spraying the inside of the cryostat chamber with commercial products such as RNaseZAP<sup>®</sup>, formulated to mitigate the harmful effects caused by such nucleases that catalyse the degradation of RNA or DNA into smaller components.

From serially-cut brain tissue sections, various histochemistry protocols, designed to allow for clear visualization of neuronal populations and white matter fiber tracks, to aid identification of the ROI, can be used on the first and last sections in the series in order to confirm presence of the ROI in-between. Typically, such stains include either Luxol Fast Blue (LFB) staining, for visualising myelin and therefore the white fibre tracts (Fig. 1A) or



Haematoxylin & Eosin (H&E) staining. Haematoxylin stains the nuclei blue, whilst eosin stains the extracellular matrix and cytoplasm pink (Fig. 1B).

Once its confirmed that the sectioned tissue contains the required ROI, an antibody-based “quick-stain” is applied to the tissue sections to visualize the cell type to isolate from the tissue using cell capture technology. This procedure entails:

1. Take glass slide-mounted tissue sections out of the -80°C freezer and air-dry them in a class II cabinet for 30 minutes
2. Ensure that all condensation has evaporated before continuing
3. Lightly wet a layer of paper towel and place inside a staining tray
4. Once the tissue sections are dry, trace around each section with a hydrophobic marker pen
5. Rinse each section with TBST (a mixture of tris-buffered saline (TBS) and Polysorbate 20, also known as Tween 20) for 3 x 5 minutes
6. Tip off the excess TBST and add pre-vortexed 5% blocking serum (horse) in TBST (1% Tween) for 30 minutes at room temperature (RT)
7. After the blocking step, tip off excess blocking serum and add pre-vortexed and centrifuged primary antibody at an optimal concentration, with the antibody diluted in TBST; incubate for 2 hours at RT in the class II cabinet
8. Following this incubation period, tip off the excess primary antibody solution and add the solution containing the species-specific horseradish peroxidase (HRP)-conjugated secondary antibody at a concentration of 1:200, diluted in TBS and incubate for 1 hour at RT


9. Tip off the excess secondary antibody solution and then wash the sections in phosphate buffered saline (PBS) for 3 x 5 minutes
10. Remove the excess PBS and then apply the chromogenic substrate TMB (3,3',5,5'-Tetramethylbenzidine) for 10 minutes at RT; note that TMB is light sensitive so light exposure should be minimised
11. Wash sections briefly with nuclease-free water
12. Use immediately for single cell isolation

From such stained sections, the cells of interest are then captured using a cell capture system, such as an LCM device. This involves using a laser to cut around a cell and then using a catapult system to collect the cell into an Eppendorf tube (Fig. 2). When using the P.A.L.M. MicroBeam Laser-Capture Microdissection system coupled to an inverted Zeiss microscope (Axiovert 200M; Carl Zeiss, Oberkochen, Germany), the procedure involves:

1. Tissue sections should be cut at 20µm thick or less to allow laser-assisted microdissection to work optimally
2. Apply the “quick-stain” methodology (see above) to visualize the cell population of interest
3. Turn on the equipment in the following order: Mains (extension lead), computer and then the power supply of the LCM; select “Zeiss” programme from desktop
4. To insert a tissue section slide click the  icon
5. To navigate to a cell click on the compass  icon
6. Insert a 0.2ml Eppendorf tube into the tube collector with the cap facing down
7. Select the “autocut” option, or select “Settings” à “Preferences” à “Laser” à Select and subsequently adjust the minimum diameter of the laser beam of the LCM


microscope (between 7.5  $\mu\text{m}$  and 30  $\mu\text{m}$ ), depending on size of cell (20  $\mu\text{m}$  is normally required for larger neurons)

8. To test settings, draw a large random spiral in an area of the tissue lying outside the ROI; adjust the settings to obtain a smooth cut with the laser set at the minimum possible “energy cut” setting to avoid scorching intended cells


9. Click  icon to access “cap move” interface; select “cap 1” and then click the



for drawing around the cell; ensure you draw closely around each cell but leave a slight margin to ensure that the cell itself is not damaged by the laser-evoked energy

10. Click the  icon to start the laser cutting

11. Once the first cutting has finished click “cap 2” on the “cap move” interface and then draw around the second cell to repeat the process

12. To remove the tube from the device, click the  icon

13. Centrifuge the collected cells for 10 minutes at 12,000 rotations per minute

14. Place the tubes on ice and commence with molecular analytical methods immediately

This procedure described here uses an LCM device that catapults the target cell into the adhesive cap of a microfuge tube. An alternative system on offer rather drops the specimen into the tube using gravity. In this case, sections are placed on specialized plastic membrane slides, where the membrane acts as a stabilizing scaffold.

Although no systematic studies have been performed so far to conclusively demonstrate this, concern exists that LCM-induced scorching may induce false mutations in

samples. However, the most prominent concern relating to the use of LCM is the cost for acquiring such a device that places single cell studies out of reach for most labs. A more economical option for cell capture from tissue, which also overcomes the issue relating to inadvertent laser-evoked scorching of the cell's borders, was recently introduced, known as a "Unipick"<sup>TM</sup> apparatus (Fig. 3). This system uses the cutting edge of a glass capillary tube to cut out the cell of interest from the surrounding tissue before vacuum suction is applied to capture the cell into the same glass capillary tube, from where it can be flushed into a microfuge tube. In our hands, we have found that the system allows more precise control over an LCM apparatus for obtaining a specific cell, thereby avoiding contaminating the sample with unwanted material such as surrounding glial cells. However, the system can only reliably cut through tissue sections of 15µm thick or less, which could be problematic if working on rare specimens provided by a collaborating lab (hence the receiving lab had no control over preparing the sections for subsequent cell isolation studies). Furthermore, we have also found that the tissue section needs to be constantly hydrated with sterile buffer containing a very small amount of detergent (e.g. Tween-20) for its cutting function to work effectively. In this regard, care should be taken to remove this bathing solution from the sample (i.e. through centrifugation) before commencing with downstream molecular analyses.

## **5.2 Mitochondrial copy number variation and measurement of mtDNA deletion levels**

MtDNA CN refers to the number of copies of the mitochondrial genome present in a cell.

mtDNA CN is typically higher in active cells such as neurons and muscle cells, but also varies on an intercellular basis [87]. Measuring mtDNA CN is a useful tool for identifying changes in rates of mitochondrial biogenesis and mitophagy in PD.



A commonly used technique for measuring mtDNA CN and mtDNA deletion levels is through the use of quantitative real-time PCR (qPCR). In this technique, quantifying expression levels of a stable mitochondrial gene *mtND1* against *mtDN4*, a mitochondrial gene that is deleted in >95% of mutated mtDNA molecules [88] can be used to measure the number of w/t molecules and molecules harbouring deletions to give an estimation of heteroplasmy levels. Alternatively, the expression levels of *mtND1* can be measured alongside the levels of a nuclear housekeeping gene such as *B2M* to determine mitochondrial CN per cell. Below we provide a stepwise methodology for single neuron (post-mortem brain) mtDNA CN analysis, as per our previously published paper [35].

To quantify mtDNA CN, commonly used technique by which to measure mtDNA CN is through quantitative real-time PCR (qPCR). This technique allows several pieces of information to be gained from each cell with deletion levels and total copies relative to nuclear DNA to be assayed together in a multiplex reaction [88]. Where a multi-cell population is used nuclear DNA must be quantified using levels of a nuclear housekeeping gene such as *B2M* to determine mitochondrial CN per cell. However, in instances where a single cell can be assured per reaction, this is not necessary. By utilising primer and probe sets localized in different regions of the mtDNA, data can be obtained regarding the number of molecules per cell which are incomplete (or negative for a particular sequencing region). A large proportion (>95%) of deleted mtDNA molecules are missing a region between  $O_H$  and  $O_L$ , termed the “common deletion” [89-91]. Due to their strategic location it is believed that these are generated during replication [17]. Thus, by selecting two sets of primers and probe sets, *mtDN4* in the deleted region and *mtND1* on the other side of the circle as a control, relative total mtDNA CN and deletion heteroplasmy levels can be calculated for

multiple single cells. Below we provide a stepwise methodology for single neuron (post-mortem brain) mtDNA CN analysis, as previously published [70, 92].

Equipment required:

1. A qPCR machine
2. Variable temperature heat block or thermocycler
3. A spectrometer to check DNA concentration
4. A vortex mixer
5. A set of calibrated pipettes

Reagents:

1. mtND1 forward primer sequence: 5' -ACGCCATAAACTCTTCACCAAG- 3'
2. mtND1 reverse primer sequence: 5' -GGGTTCATAGTAGAAGAGCGATGG- 3'
3. mtND4 forward primer sequence: 5' -ACCTTGGCTATCATCACCCGAT- 3'
4. mtND4 reverse primer sequence: 5' -AGTGCGATGAGTAGGGGAAGG- 3'
5. mtND1 probe: 5' -Hex-CCCGCCACATCTACCATCACCTC- 3' (BHQ-1)
6. mtND4 probe: 5' -CY5-CAACCAGCCAGAACGCCTGAACGCA- 3' (BHQ-2)
7. A qPCR Master Mix: A range of these are available e.g. Luna<sup>®</sup> Universal Probe qPCR Master Mix (New England Biolabs). Ensure that the selected one is compatible with the qPCR machine to be used e.g. some require the inert fluorescent dye "ROX" to serve as a passive reference, while some do not
8. 1 M Tris HCl, pH 8 (Fisher Scientific)
9. Tween-20 (Sigma-Aldrich)
10. Proteinase K (20 mg/ml) (New England Biolabs)

11. RNase- and DNase-free H<sub>2</sub>O (Fisher Scientific)
12. 1.5ml, 0.5ml or 0.2ml sized tubes, suitable for use in a heat block or thermocycler
13. 96-well plates, suitable for the qPCR machine available for these experiments
14. Plate seals, suitable for the qPCR machine available for these experiments
15. Human mtDNA or total DNA sample or at least one human-type cell

Reagents required for generating the standard curve:

1. mtND1 forward primer sequence: 5' -CAGCCGCTATTAAAGGTTTCG- 3'
2. mtND1 reverse primer sequence: 5'-AGAGTGCGTCATATGTTGTTC- 3'
3. mtND4 forward primer sequence: 5'- ATCGCTCACACCTCATATCC -3'
4. mtND4 reverse primer sequence: 5'-TAGGTCTGTTTGTTCGTAGGC-3'
5. A thermocycler
6. PCR tubes
7. A qPCR Master Mix e.g. Phusion<sup>®</sup> High-Fidelity DNA Polymerase (New England Biolabs)
8. Deoxynucleotides (dNTPs) (10 mM) (New England Biolabs)
9. An agarose gel tank
10. Agarose powder (Fisher Scientific)
11. Tris/Borate/EDTA (TBE) buffer (Fisher Scientific)
12. A nucleic acid stain e.g. ethidium bromide (ETBr) (10 mg/ml) or SYBR Safe Stain (Fisher Scientific)
13. UV or blue light gel visualizer
14. A DNA size marker (New England Biolabs)
15. A PCR clean-up kit e.g. Monarch<sup>®</sup> PCR & DNA Cleanup Kit (New England Biolabs)

Additional things to consider before starting such experiments:

1. Ensure that the probe labels are of suitable fluorescence for the qPCR machine to be used and also that the correct quenchers have been selected, for example Cy5, BHQ2 may be replaced by Fam, BHQ1 if required.
2. Contamination is the mostly likely problem one encounters when working with low template material such as single cells. If space is available, consider keeping a clean area for final set up of the qPCR reactions away from tissue preparation and standard curve preparation areas, where there could be high levels of contaminating material. If possible, also have a “clean” set of pipettes for generating the qPCR data.

You should ensure that you can produce consistent standard curves and that primers and probe sets produce the same standard curves in single and multiplex reactions before proceeding to mtDNA CN analysis of single cells. In order to calculate mtDNA CN directly a standard curve of known mtDNA CN is required. This can also be used to check that reactions work in a linear manner and that reactions are consistent across plates. A reliable standard curve also offers a way to check primers and optimize technique before working with precious samples.

The relative standard curve method:

1. A standard curve consists of 4 points (or 4 “standards”) that are generated by means of a serial 10-fold dilution of DNA
2. A small amount of starting human mtDNA is required for generating standard curve material. This can be obtained from any w/t human cultured cells or tissue using a

genomic DNA preparation kit such as Monarch<sup>®</sup> Genomic DNA Purification Kit (New England Biolabs)

3. Begin by diluting DNA in RNase and DNase-free H<sub>2</sub>O to have 20 µl containing 20x10<sup>5</sup> DNA copies that must contain DNA for both ND1 and ND4
4. In a fresh tube add 2 µl of the above DNA to 18 µl RNase and DNase-free H<sub>2</sub>O
5. Repeat this another 2x to produce 4 standards, which will produce CNs of 5x10<sup>5</sup>, 5x10<sup>4</sup>, 5x10<sup>3</sup> and 5x10<sup>2</sup> per qPCR reaction
6. Standard curves are carried out in triplicate and DNA is used to make serial dilutions for the standard curve. So for each standard curve point at least 20 µl of DNA must be prepared
7. Prepare the primers following the manufacturer's instructions, to generate 100µM stocks; store these at -20°C till further use
8. From the primer stocks, prepare working dilutions of primers: 10 µM, by 1/10 dilution in RNase and DNase -free H<sub>2</sub>O to avoid contamination of stocks whilst working. Always prepare at least 10% more than is required
9. Set up the qPCR reactions for MTND1 and MTND4 on ice following the manufacturer's instructions, e.g. for Phusion<sup>®</sup> High-Fidelity DNA Polymerase (New England Biolabs) the reaction is as follows: 50-250 ng/ml DNA template, 5 µl 5x reaction buffer, 0.8 µl forward primer, 0.8 µl reverse primer, 0.6 µl dNTPs, 0.2 µl phusion, made up to 25 µl with RNase and DNase-free H<sub>2</sub>O. ensure that all samples are mixed well by vortexing
10. For one standard curve qPCR run, 12x reactions and 1x NTC is needed; add 5 µl standard curve DNA to the appropriate wells and add 5 µl RNase and DNase-free H<sub>2</sub>O to the NTC

11. Cover the plate with adhesive seal and then load the plate into the qPCR machine
12. Perform the PCR reaction in a thermocycler by applying the following cycles: 1 minute at 98°C followed by 30 cycles, 98°C for 30 secs, 58°C 30 secs, 72 °C for 1 minute
13. Input the standard curve values into the qPCR computer software and calculate the standard curve values using generated CT (cycle threshold; see below) values
14. This reaction should produce a product of 1 kb for each gene which should be checked on an agarose gel: Dissolve 1 g of agarose powder in 100ml 1x TBE powder in a 500 ml glass conical flask or another suitable container (volume may vary dependent upon agarose gel tank size); heat the solution slowly in a microwave until agarose is fully dissolved in the buffer; allow the solution to cool for 5- 10 minutes until the flask can be held comfortably by hand; add ETBr (5 µl) or SYBR Safe Stain (1/10,000); pour the solution into the gel tray containing a suitably-sized comb; allow the gel to set for approximately 1 hr at RT; now place the set gel in the tank, remove the comb and cover with TBE buffer; mix 3 µl of each PCR reaction product with 1 µl of DNA loading dye; load the samples onto the gel alongside the DNA ladder; run for 45 minutes at 100 V, dependent on gel size; finally visualise using UV or a blue light box
15. One band for each primer set at the same size as the 1 kb ladder band should be visible; if multiple bands of different sizes or no band is seen, the reaction can be optimized by varying the annealing temperature by several degrees (either up or down) or by adding additional factors to the reaction, such as MgCl<sub>2</sub> or DMSO (dimethyl sulfoxide). Different polymerases have varying condition and buffer preferences so some optimization may be required to achieve the optimal results

16. Once optimal qPCR results have been achieved, the remaining reaction can be purified for downstream use. The remaining 22  $\mu$ l should be purified using a DNA clean up column such as Monarch<sup>®</sup> PCR & DNA Cleanup Kit (New England Biolabs), following the manufacturer's instructions
17. Once standard curves have been optimized, larger volumes of standards can be made and stored at 4°C to be used on multiple plates
18. Check the DNA concentration of the products on a spectrometer
19. mtDNA CN can be calculated by using the following calculation:  $\text{mtDNA CN} = (\text{DNA concentration (ng)} \times 6.02 \times 10^{23}) / ((L \times 660) \times 1 \times 10^9)$ , where L is DNA length in bp (ND1-1040bp, ND4-1072bp). A number of freely available calculators can also be found online
20. Samples can be stored at 4°C for short term (1 month) or -20°C for longer term to produce more product; these products may also be cloned into a plasmid to produce a long-term resource for generating standard curve material

Quality assurance checks:

1. Check the  $r^2$  value of the standard curve, which should be >0.95
2. Check reproducibility of the triplicate repeats, which should be within 1 standard deviation of each other
3. Check that no signal is observed in the NTC, in order to confirm no contamination of any reagents
4. ND1 and ND4 reactions should be compared in single and multiplex reactions to ensure no bias is created in multiplexing the reactions, where single and multiplex reactions should produce the same standard curves

DNA sample preparation for the qPCR reactions:

1. Prepare the lysis buffer: 50mM Tris-HCl (pH 8.0), 1% Tween-20 and 200 µg/ml proteinase K; 40 µl per sample is required
2. For one sample, 2 µl 1M Tris pH 8, 0.4 µl Tween 20, 0.4 µl Proteinase K, 37.2 µl RNase, DNase free H<sub>2</sub>O, scale up mastermix as required dependent on number of samples to be processed
3. Isolate single cells from the tissue as described above
4. Place each cell into an appropriately sized PCR tube for placing in the heating block or thermocycler
5. Incubate the tube at 55°C for 2hrs followed by 10 minutes at 95°C
6. At this stage, samples can be stored at 4°C for short term (1 month) or -20 °C for longer term

The qPCR workflow:

1. Prepare the working area and ensure that pipettes and the work bench is clean and free of any potential contamination. If a PCR hood or dedicated room is available this may further help to avoid any contamination
2. Once the reagents are fully defrosted, keep all samples and reagents on ice
3. If required, prepare the primers and probes following the manufacturer's instructions to generate 100 µM stocks; probes are light sensitive so protect these from light. Store the primers and probes at at -20°C till further use
4. Prepare the working dilutions for the primers and probes (10 µM for each), by means of a 1/10 dilution in RNase and DNase-free H<sub>2</sub>O to avoid contamination of stocks.



Always prepare at least 10% more than required, but enough for several plates can be prepared and stored at -20°C

5. Prepare map of the qPCR plate in order to optimize reactions per plate. qPCR reactions are carried out in triplicate, against the standard curve described above and also a NTC. Use of an NTC ensures that the reactions are not contaminated with other DNA
6. Calculate the qPCR reactions to be carried out, and also 12x standard curve, 1x NTC, with all samples performed in triplicate; add an additional 10% to account for pipetting errors
7. Calculate the amount of qPCR Master Mix that will be needed; this is dependent on the manufacturer's instructions, e.g. for the Luna<sup>®</sup> Universal Probe qPCR Master Mix (New England Biolabs), each sample consists of a 20 µl reaction utilizing 0.4µM primers and 0.2µM probe. In our hands, we find that 5ul of template per reaction is normally optimal, but this may need to be optimized for the exact set up to be used
8. An example of a single reaction includes 1 µl RNase and DNase-free H<sub>2</sub>O, 10 µl qPCR Master Mix, 0.8 µl of each forward and reverse primer working dilution and 0.4 µl of each probe working dilution
9. Add the Master Mix to the wells of a 96 well plate; try to avoid bubbles when pipetting the solution
10. Add 5 µl of the standard curve or the sample DNA to the wells by following the plate map. Use a fresh full tip pipette box and match each tip to each well to ensure all samples are located correctly and none are missed. Pipette the samples up and down 3x when added in order to mix the content well; however, avoid forming bubbles

11. Add 5  $\mu$ l RNase- and DNase-free H<sub>2</sub>O to the NTC wells
12. Cover the plate with an adhesive plate seal
13. The plate can be spun briefly using a centrifuge, to ensure that all reactions sit in the bottom of the wells and also to remove bubbles that might interfere with the readings
14. Load the plate into the qPCR machine; some machines may require a plate cover so ensure this is in place if required
15. Open the qPCR analysis computer software and load the correct qPCR program; this will vary between machines so check the manufacturer's instructions in order to choose correct one
16. The software program may vary dependent on the Master Mix reagent used, so follow the manufacturer's instructions, e.g. for the Luna<sup>®</sup> Universal Probe qPCR Master Mix (New England Biolabs) this is 95°C for 60 secs, followed by 45 cycles of 95°C for 15 secs each, and then finally 60°C for 30 secs
17. Set a single quantification at the end of each cycle for the probes used, namely Hex and Cy5
18. Start the PCR reaction through the software interface
19. Once the reactions are finished, discard the plate and turn off the machine

Data analysis:

1. Analyse the data using the machine's software; this will vary across machines so follow manufacturer's guide
2. Ensure that the plate map is loaded into the software so that each well is identified; this can usually be done before a run and saved or updated later

3. Input the standard curve information
4. To confirm an absence of DNA contamination, ensure that no signal is seen in the no template control wells

Results can be obtained in two ways:

- (1) The CT represents the cycle number at which the fluorescent signal rises above the background threshold and thus indicates the point at which the qPCR reaction begins exponential growth, which is dependent on the amount of starting material
- (2) Reactions can also be given as a relative value dependent on their CT value, to compared to the standard curve
  - a) Collect the data for the samples tested, where these can usually be exported as a CSV (comma-separated value) file and the opened in Microsoft Excel for further analysis
  - b) Check the sample triplicate readings; any significant outliers caused by errors may need to be removed
  - c) mtDNA CN can then be analysed by comparing CT values for MTND1 across different samples
  - d) These values can normally be generated within the qPCR machine analysis software through direct reference to the standard curve
  - e) It is important to remember to account for dilutions as only 5  $\mu$ l is used per reaction from a starting 35  $\mu$ l. Therefore, mtDNA CN per reaction represents a 7<sup>th</sup> of the total cellular DNA
  - f) To calculate mtDNA deletions, use the  $\Delta$ ct method
  - g) Relative mtDNA CN =  $2^{-\Delta CT}$ , where  $\Delta CT = CT_{ND1} - CT_{ND4}$

h) The calculated value can then be converted to a percentage deletion level

Limitations of qPCR include measurement error when processing samples [87]. Starting DNA concentration is critical for copy number assays as low DNA concentrations can lead to increases in measurement error [88]. mtDNA heteroplasmy levels can also impact mtDNA CN assays with accuracy of the *MTND1/MTND4* assay decreasing when lower levels of deleted mtDNA molecules are present [88]. This makes studying mtCN challenging at a single cell level due to low starting concentrations of mtDNA and potentially high levels of heteroplasmy in individual cells. It is also difficult to measure subtle changes in mtCN or heteroplasmy levels with current qPCR technologies [88].

Performing qPCR in triplicate is standard but may not provide enough power to detect subtle changes in heteroplasmy levels, particularly when working with low starting mtDNA concentrations [88]. Using homogenate tissue samples to quantify mtDNA CN in a specific cell type also carries the risk of measuring CN from other cell types, such as glia, that reside in the same tissues [70].

There are a number of alternative methods to assess mtDNA copy number, many of these have downsides such as low throughput or high cost, but do offer an excellent way to confirm copy number and heteroplasmy differences on a smaller scale to compliment and confirm data that may have been obtained through qPCR. As mentioned above, mtDNA can be observed by immunofluorescence but this may be difficult to achieve when working with single cells derived from tissue samples. A more feasible method is southern blotting where total DNA is separated by electrophoresis and then blotted onto a membrane where selected regions can be identified by sequence-specific radioactively-labelled probes [92]. This method potentially offers a way to confirm data achieved by means of qPCR; however, at a

single cell level the genomic starting material is very low and high accuracy is needed to observe differences. In addition, this method is relatively low throughput, time consuming and requires the use of radioactive labels. Other alternatives include microarray analysis and whole exome sequencing however, such methods are likely to be much more expensive and require specialist equipment.

An emerging alternative technique to qPCR is digital droplet PCR (ddPCR) that is more sensitive and can work with lower starting concentrations of DNA. Furthermore, ddPCR does not rely on the use of external standards and is thus considered more accurate than qPCR as there is a reduced occurrence of error rates. It has been shown that variation in copy number results can be seen with changes in DNA extraction kits and methods thus the key thing when setting up such experiments is to ensure a robust method is designed and tested before samples are tested and that all reagents and methods are kept the same for all samples. In addition, a number of other qPCR assays are available to allow analysis of mutation load such as the Random Mutation Capture (RMC) assay [93] and long-range PCR assays [94].

### **Conclusions and future directions**

Over the last 25 years significant progress has been made into investigating the link between mitochondrial dysfunction and the progression of PD. This includes studies examining the impact of somatic mutations within mtDNA. Given the potential and causal role of mtDNA variation in PD pathogenesis, understanding reasons for preferential accumulation of mtDNA deletions and differential patterns of mtDNA CN variation across different cell populations as a result of PD appears crucial in light of recent work which highlighted cell-specific responses to PD.

Whilst work is ongoing in this area to characterise where deletions occur in the mitochondrial genome and the effects of these deletions on mitochondrial function, single cell studies are not without limitations. The low starting yields of mtDNA obtained from a single neuron combined with DNA degradation during storage can create difficulties in amplifying and sequencing mtDNA. DNA degradation is also likely to occur in post-mortem brain tissue that is non-fixed. Studies on post-mortem tissue in PD are further compounded where vulnerable neurons have already died and those remaining may exhibit some resistance to degeneration. Furthermore, any errors in sampling methodology or sequencing could lead to spurious associations between mtDNA variants and PD. Regardless of such limitations, studying somatic mutations at a single neuron level continue to provide significant insight into how mtDNA deletions differ between individual neurons and between different neuronal populations in PD, to promise identification of durable targets to exploit in therapeutic approaches.

**Abbreviations used:**

$\alpha$ -synuclein,  $\alpha$ -SYN; Acetylcholine, ACh; Adenosine triphosphate, ATP; Choline acetyltransferase, ChAT; Copy number, CN; Cycle threshold, CT; Cytochrome c oxidase, COX; Deep-brain stimulation, DBS; Dimethyl sulfoxide, DMSO; Displacement, D; Digital droplet PCR, ddPCR; Dopamine transporter, DAT; Electron transport chain, ETC; Ethidium bromide, ETBr; Haematoxylin & Eosin, H&E; Heavy, H; Horseradish peroxidase, HRP; 5-hydroxytryptamine, 5-HT; Laser capture microdissection, LCM; Lewy bodies, LBs; Lewy neurites, LNs; Light, L; Light- (or lagging-) strand, LC-RNA; Locus coeruleus, LC; Luxol Fast Blue, LFB; 1-methyl-4-phenylpyridinium, MPP<sup>+</sup>; Mitochondrial, mt; Non-coding regions, NCR; Norepinephrine, NE; Oxidative phosphorylation, OXPHOS; Pedunculopontine nucleus, PPN; Phosphate buffered

saline, PBS; Polymerase  $\gamma$ , POLG; Random Mutation Capture, RMC; Region of interest, ROI; Reactive oxygen species, ROS; Ribosomal RNA, rRNA; Room temperature, RT; Single nucleotide polymorphisms, SNPs; Substantia Nigra pars compacta, SNpc; Subthalamic nucleus, STN; 3,3',5,5'-Tetramethylbenzidine, TMB; Transcription factor A, mitochondrial, TFAM; Transfer RNA, tRNA; Tris-buffered saline, TBS; Vascular endothelial growth factor, VEGF; Wild-type, w/t

## References

1. Martin WF, Garg S, Zimorski V (2015) Endosymbiotic theories for eukaryote origin. *Philos Trans R Soc Lond B Biol Sci* 370:20140330
2. Papa S, Martino PL, Capitanio G et al (2012) The oxidative phosphorylation system in mammalian mitochondria. *Adv Exp Med Biol* 942:3–37
3. Raule N, Sevini F, Li S et al (2014) The co-occurrence of mtDNA mutations on different oxidative phosphorylation subunits, not detected by haplogroup analysis, affects human longevity and is population specific. *Aging Cell* 13:401–407
4. Gómez-Durán A, Pacheu-Grau D, López-Gallardo E et al (2010) Unmasking the causes of multifactorial disorders: OXPHOS differences between mitochondrial haplogroups. *Hum Mol Genet* 19:3343–3353
5. Lapkouski M, Hällberg BM (2015) Structure of mitochondrial poly(A) RNA polymerase reveals the structural basis for dimerization, ATP selectivity and the SPAX4 disease phenotype. *Nucleic Acids Res* 43:9065–9075

6. Kasamatsu H, Robberson DL, Vinograd J (1971) A novel closed-circular mitochondrial DNA with properties of a replicating intermediate. *Proc Natl Acad Sci USA* 68:2252–2257
7. Nicholls TJ, Minczuk M (2014) In D-loop: 40 Years of Mitochondrial 7S DNA. *Exp Gerontol* 56:175–181
8. He J, Mao C-C, Reyes A, et al (2007) The AAA+ protein ATAD3 has displacement loop binding properties and is involved in mitochondrial nucleoid organization. *J Cell Biol* J Cell Biol 176:141–146
9. Antes A, Tappin I, Chung S, et al (2010) Differential regulation of full-length genome and a single-stranded 7S DNA along the cell cycle in human mitochondria. *Nucleic Acids Res* 38:6466–6476
10. Annex BH, Williams RS (1990) Mitochondrial DNA structure and expression in specialized subtypes of mammalian striated muscle. *Mol Cell Biol* 10:5671–5677
11. Reyes A, Rusecka J, Tońska K et al (2020) RNase H1 regulates mitochondrial transcription and translation via the degradation of 7S RNA. *Front Genet* 10:1393
12. Akman G, Desai R, Bailey LJ et al (2016) Pathological ribonuclease H1 causes R-loop depletion and aberrant DNA segregation in mitochondria. *Proc Natl Acad Sci USA* 113:E4276–4285
13. Fusté JM, Wanrooij S, Jemt E et al (2010) Mitochondrial RNA polymerase is needed for activation of the origin of light-strand DNA replication. *Mol Cell* 37:67–78
14. Wanrooij S, Fusté JM, Farge G et al (2008) Human mitochondrial RNA polymerase primes lagging-strand DNA synthesis in vitro. *Proc Natl Acad Sci USA* 105:11122–11127
15. Raha S, Robinson BH (2000) Mitochondria, oxygen free radicals, disease and ageing. *Trends Biochem Sci* 25:502–508



16. Lin MT, Beal MF (2006) Mitochondrial dysfunction and oxidative stress in neurodegenerative diseases. *Nature* 443:787–795
17. Tuppen HA, Blakely EL, Turnbull DM et al (2010) Mitochondrial DNA mutations and human disease. *Biochim Biophys Acta* 1797:113–128
18. Kadenbach B, Münscher C, Frank V et al (1995) Human aging is associated with stochastic somatic mutations of mitochondrial DNA. *Mutat Res* 338:161–172
19. Khrapko K, Turnbull D (2014) Mitochondrial DNA mutations in aging. *Prog Mol Biol Transl Sci* 127:29–62
20. Elson JL, Samuels DC, Turnbull DM, et al (2001) Random intracellular drift explains the clonal expansion of mitochondrial DNA mutations with age. *Am J Hum Genet* 68:802–806
21. Chinnery PF, Samuels DC, Elson JL et al (2002) Accumulation of mitochondrial DNA mutations in ageing, cancer, and mitochondrial disease: Is there a common mechanism? *Lancet* 360:1323–1325
22. Kowald A, Kirkwood TBL (2018) Resolving the enigma of the clonal expansion of mtDNA deletions. *Genes (Basel)* 9
23. Moustafa AA, Chakravarthy S, Phillips JR et al (2016) Motor symptoms in Parkinson's disease: A unified framework. *Neurosci Biobehav Rev* 68:727–740
24. Balestrino R, Martinez-Martin P (2017) Neuropsychiatric symptoms, behavioural disorders, and quality of life in Parkinson's disease. *J Neurol Sci* 373:173–178
25. Alexander GE (2004) Biology of Parkinson's disease: Pathogenesis and pathophysiology of a multisystem neurodegenerative disorder. *Dialogues Clin Neurosci* 6:259–280

26. Trojanowski JQ1, Goedert M, Iwatsubo T et al (1998) Fatal attractions: Abnormal protein aggregation and neuron death in Parkinson's disease and Lewy body dementia. *Cell Death Differ* 5:832–837
27. Braak H, Del Tredici K, Rüb U et al (2003) Staging of brain pathology related to sporadic Parkinson's disease. *Neurobiol. Aging* 24:197–211
28. Hansen C, Angot E, Bergström A-L et al (2011)  $\alpha$ -Synuclein propagates from mouse brain to grafted dopaminergic neurons and seeds aggregation in cultured human cells. *J Clin Invest* 121:715–725
29. Desplats P, Lee HJ, Bae EJ et al (2009) Inclusion formation and neuronal cell death through neuron-to-neuron transmission of alpha-synuclein. *Proc Natl Acad Sci USA* 106:13010–13015
30. Luk KC, Song C, O'Brien P et al (2009) Exogenous alpha-synuclein fibrils seed the formation of Lewy body-like intracellular inclusions in cultured cells. *Proc Natl Acad Sci USA* 106:20051–20056
31. Luk KC, Kehm V, Carroll J et al (2012) Pathological  $\alpha$ -synuclein transmission initiates Parkinson-like neurodegeneration in non-transgenic mice. *Science* 338:949–953
32. Mesulam MM, Mufson EJ, Wainer BH et al (1983) Central cholinergic pathways in the rat: An overview based on an alternative nomenclature (Ch1-Ch6). *Neuroscience* 10:1185–1201
33. Rinne JO, Ma SY, Lee MS et al (2008) Loss of cholinergic neurons in the pedunculopontine nucleus in Parkinson's disease is related to disability of the patients. *Parkinsonism Relat Disord* 14:553–557

34. Pienaar IS, Elson JL, Racca C et al (2013) Mitochondrial abnormality associates with type-specific neuronal loss and cell morphology changes in the pedunclopontine nucleus in Parkinson disease. *Am J Pathol* 183:1826–1840
35. Bury AG, Pyle A, Elson JL et al (2017) Mitochondrial DNA changes in pedunclopontine cholinergic neurons in Parkinson disease. *Ann Neurol* 82:1016–1021
36. Standaert D, Saper C, Rye D et al (1986) Colocalization of atriopeptin-like immunoreactivity with choline acetyltransferase- and substance—P-like immunoreactivity in the pedunclopontine and laterodorsal tegmental nuclei in the rat. *Neuroscience* 382:163–168
37. Austin M, Rice P, Mann J et al (1995) Localization of corticotropin-releasing hormone in the human locus coeruleus and pedunclopontine tegmental nucleus: An immunocytochemical and *in situ* hybridization study. *Neuroscience* 64:713–727
38. Mineff EM, Popratiloff A, Romansky R et al (1998) Evidence for a possible glycinergic inhibitory neurotransmission in the midbrain and rostral pons of the rat studied by gethyrin. *Arch Physiol Biochem* 106:210–220
39. Wang HI, Morales M (2009) Pedunclopontine and laterodorsal tegmental nuclei contain distinct populations of cholinergic, glutamatergic, and GABAergic neurons in the rat. *Eur J Neurosci* 29:340–358
40. Martinez-Gonzalez C, Wang HL, Micklem BR et al (2012) Subpopulations of cholinergic, GABAergic and glutamatergic neurons in the pedunclopontine nucleus contain calcium-binding proteins and are heterogeneously distributed. *Eur J Neurosci* 35:723–734
41. Pienaar IS, van de Berg W (2013) A non-cholinergic neuronal loss in the pedunclopontine nucleus of toxin-evoked Parkinsonian rats. *Exp Neurol* 248:213–223

42. D'Onofrio S, Kezunovic N, Hyde JR et al (2015) Modulation of gamma oscillations in the pedunculo-pontine nucleus by neuronal calcium sensor protein-1: Relevance to schizophrenia and bipolar disorder. *J Neurophysiol* 113:709–719
43. Gutt NK, Winn P (2016) The pedunculo-pontine tegmental nucleus-A functional hypothesis from the comparative literature. *Mov Disord* 31:615–624
44. Jiang H, Song N, Jiao Q et al (2019) Iron pathophysiology in Parkinson's disease. *Adv Exp Med Biol* 1173:45–66
45. Lewis FW, Fairouz S, Elson JL et al (2020) Novel 1-hydroxypyridin-2-one metal chelators prevent and rescue ubiquitin proteasomal-related neuronal injury in an in vitro model of Parkinson's disease. *Arch Toxicol* 94:813–831
46. Mochizuki H, Choong CJ, Baba K (2020) Parkinson's disease and iron. *J Neural Transm* 127:181–187
47. Shamoto-Nagai M, Maruyama W, Yi H et al (2006) Neuromelanin induces oxidative stress in mitochondria through release of iron: Mechanism behind the inhibition of 26S proteasome. *J Neural Transm* 113:633–644
48. Zecca L, Stroppolo A, Gatti A et al (2004) The role of iron and copper molecules in the neuronal vulnerability of locus coeruleus and substantia nigra during aging. *Proc Natl Acad Sci USA* 101:9843–9848
49. Zucca FA, Bellei C, Giannelli S et al (2006) Neuromelanin and iron in human locus coeruleus and substantia nigra during aging: Consequences for neuronal vulnerability. *J Neural Transm* 113:757–767
50. Pienaar IS, Lee CH, Elson JL et al (2015) Deep-brain stimulation associates with improved microvascular integrity in the subthalamic nucleus in Parkinson's disease. *Neurobiol Dis* 74:392–405

51. Booth HDE, Hirst WD, Wade-Martins R (2017) The role of astrocyte dysfunction in Parkinson's disease pathogenesis. *Trends Neurosci* 40:358–370
52. Sofroniew MV, Vinters HV (2010) Astrocytes: Biology and pathology. *Acta Neuropathol* 119:7–35
53. Zhang Y, Sloan SA, Clarke LE et al (2016) Purification and characterization of progenitor and mature human astrocytes reveals transcriptional and functional differences with mouse. *Neuron* 89:37–53
54. Streit WJ, Mrak RE, Griffin WST (2004) Microglia and neuroinflammation: A pathological perspective. *J Neuroinflammation* 1:14
55. Gelders G, Baekelandt V, Van der Perren A (2018) Linking neuroinflammation and neurodegeneration in Parkinson's disease. *J Immunol Res* 2018:4784268–4784212
56. George S, Rey NL, Tyson T et al (2019) Microglia affect  $\alpha$ -synuclein cell-to-cell transfer in a mouse model of Parkinson's disease. *Mol Neurodegener* 14:34
57. Ballard PA, Tetrad JW, Langston JW (1985) Permanent human parkinsonism due to 1-methyl-4-phenyl-1,2,3,6-tetrahydropyridine (MPTP): Seven cases. *Neurology* 35:949–956
58. Choi SJ, Panhelainen A, Schmitz Y et al (2015) Changes in neuronal dopamine homeostasis following 1-methyl-4-phenylpyridinium (MPP+) exposure. *J Biol Chem* 290:6799–6809
59. Nicklas WJ, Vyas I, Heikkila RE (1985) Inhibition of NADH-linked oxidation in brain mitochondria by 1-methyl-4-phenyl-pyridine, a metabolite of the neurotoxin, 1-methyl-4-phenyl-1,2,5,6-tetrahydropyridine. *Life Sci* 36:2503–2508
60. Javitch JA, D'Amato RJ, Strittmatter SM et al (1985) Parkinsonism-inducing neurotoxin, N-methyl-4-phenyl-1,2,3,6-tetrahydropyridine: Uptake of the metabolite N-methyl-4-

- phenylpyridine by dopamine neurons explains selective toxicity. *Proc Natl Acad Sci USA* 82:2173–2177
61. Gainetdinov RR, Fumagalli F, Jones SR et al (1997) Dopamine transporter is required for in vivo MPTP neurotoxicity: Evidence from mice lacking the transporter. *J Neurochem* 69:1322–1325
  62. Martí Y, Matthaeus F, Lau T et al (2017) Methyl-4-phenylpyridinium (MPP+) differential affects monoamine release and reuptake in murine embryonic stem cell-derived dopaminergic and serotonergic neurons. *Mol Cell Neurosci* 83:37–45
  63. Shannak K, Rajput A, Rozdilsky B et al (1994) Noradrenaline, dopamine and serotonin levels and metabolism in the human hypothalamus: Observations in Parkinson's disease and normal subjects. *Brain Res* 639:33–41
  64. Kish SJ, Tong J, Hornykiewicz O et al (2008) Preferential loss of serotonin markers in caudate versus putamen in Parkinson's disease. *Brain* 131:120–131
  65. Schapira AHV, Cooper JM, Dexter D et al (1990) Mitochondrial complex I deficiency in Parkinson's disease. *J Neurochem* 54:823–827
  66. Krueger MJ, Singer TP, Casida JE et al (1990) Evidence that the blockade of mitochondrial respiration by the neurotoxin 1-methyl-4-phenylpyridinium (MPP+) involves binding at the same site as the respiratory inhibitor, rotenone. *Biochem Biophys Res Commun* 169:123–128
  67. Sherer TB, Betarbet R, Testa CM et al (2003) Mechanism of toxicity in rotenone models of Parkinson's disease. *J Neurosci* 23:10756–10764
  68. Betarbet R, Sherer TB, McKenzie G et al (2000) Chronic systemic pesticide exposure reproduces features of Parkinson's disease. *Nat Neurosci* 3:1301–1306

69. Hudson G, Nalls M, Evans JR et al (2013) Two-stage association study and meta-analysis of mitochondrial DNA variants in Parkinson disease. *Neurology* 80:2042–2048
70. Pyle A, Anugraha H, Kurzawa-Akanbi M et al (2016) Reduced mitochondrial DNA copy number is a biomarker of Parkinson's disease. *Neurobiol Aging* 38:216.e7–216.e10
71. Schapira AH (2008) Mitochondria in the aetiology and pathogenesis of Parkinson's disease. *Lancet Neurol* 7:97–109
72. Schapira AH, Cooper JM, Dexter D et al (1989) Mitochondrial complex I deficiency in Parkinson's disease. *Lancet* 1:1269
73. Parker WD Jr., Boyson SJ, Parks JK (1989) Abnormalities of the electron transport chain in idiopathic Parkinson's disease. *Ann Neurol* 26:719–723
74. Mizuno Y, Ohta S, Tanaka M et al (1989) Deficiencies in complex I subunits of the respiratory chain in Parkinson's disease. *Biochem Biophys Res Commun* 163:1450–1455
75. Coppede F, Migliore L (2015) DNA damage in neurodegenerative diseases. *Mutat Res* 776:84–97
76. Swerdlow RH, Parks JK, Miller SW et al (1996) Origin and functional consequences of the complex I defect in Parkinson's disease. *Ann Neurol* 40:663–671
77. Kraytsberg Y, Kudryavtseva E, McKee AC et al (2006) Mitochondrial DNA deletions are abundant and cause functional impairment in aged human substantia nigra neurons. *Nat Genet* 38:518–520
78. Yao Z, Wood NW (2009) Cell death pathways in Parkinson's disease: Role of mitochondria. *Antioxid Redox Signal* 11:2135–2149
79. Bender A, Krishnan KJ, Morris CM et al (2006) High levels of mitochondrial DNA deletions in substantia nigra neurons in aging and Parkinson disease. *Nat Genet* 38:515–517

80. Coxhead J, Kurzawa-Akanbi M, Hussain R et al (2015) Somatic mtDNA variation is an important component of Parkinson's disease. *Neurobiol Aging* 38:217.e1-217.e6
81. Dölle C, Flønes I, Nido GS et al (2016) Defective mitochondrial DNA homeostasis in the substantia nigra in Parkinson disease. *Nat Commun* 7:13548.
82. Müller-Nedebock AC, Brennan RR, Venter M et al (2019) The unresolved role of mitochondrial DNA in Parkinson's disease: An overview of published studies, their limitations, and future prospects. *Neurochem Int* 129:104495
83. Ekstrand MI, Terzioglu M, Galter D et al (2007) Progressive parkinsonism in mice with respiratory-chain-deficient dopamine neurons. *Proc Natl Acad Sci USA* 104:1325–1330
84. Müller SK, Bender A, Laub C et al (2013) Lewy body pathology is associated with mitochondrial DNA damage in Parkinson's disease. *Neurobiol Aging* 34:2231–2233
85. Neuhaus JFG, Baris OR, Hess S et al (2014) Catecholamine metabolism drives generation of mitochondrial DNA deletions in dopaminergic neurons. *Brain* 137:354–365
86. Weissig V (2020) Drug development for the therapy of mitochondrial diseases. *Trends Mol Med* 26:40–57
87. Guyatt AL, Brennan RR, Burrows K et al (2019) A genome-wide association study of mitochondrial DNA copy number in two population-based cohorts. *Hum Genomics* 13:6
88. Grady JP, Murphy JL, Blakely EL et al (2014) Accurate measurement of mitochondrial DNA deletion level and copy number differences in human skeletal muscle. *PLoS One* 9:e114462
89. Reeve AK, Krishnan KJ, Turnbull DM (2008) Age related mitochondrial degenerative disorders in humans. *Biotechnol J* 3:750–756
90. Damas J, Samuels DC, Carneiro J et al (2014) Mitochondrial DNA rearrangements in health and disease – A comprehensive study. *Hum Mutat* 35:1–14



91. Belmonte FR, Martin JL, Frescura K et al (2016) Digital PCR methods improve detection sensitivity and measurement precision of low abundance mtDNA deletions. *Sci Rep* 6:25186
92. He L, Chinnery PF, Durham SE et al (2002) Detection and quantification of mitochondrial DNA deletions in individual cells by real-time PCR. *Nucleic Acids Res* 30:e68
93. Vermulst M, Bielas JH, Loeb LA (2008) Quantification of random mutations in the mitochondrial genome. *Methods* 46:263–268
94. Sanders LH, Rouanet JP, Howlett EH et al (2018) Newly revised protocol for quantitative PCR-based assay to measure mitochondrial and nuclear DNA damage. *Curr Protoc Toxicol* 76:e50